5th CIRP Conference on High Performance Cutting 2012

Influence of the Honed Cutting Edge on Tool Wear and Surface Integrity in Slot Milling of 42CrMo4 Steel

Berend Denkena[a], Jens Koehler[a], Michael Rehe[a]*

aInstitute of Production Engineering and Machine Tools, An der Universität 2, 30823 Garbsen, Germany
* Corresponding author. Tel.: +49 (0)511 762 18006; fax: +49 (0)511 762 18006; E-mail address: rehe@ifw.uni-hannover.de

Abstract

The cutting edge microgeometry has a significant influence on the wear behavior of cutting tools and therefore on the machining performance. To investigate the effect of tailored cutting edge microgeometries, a detailed geometrical description of different cutting edge designs is necessary. The cutting edge profile is analyzed with respect to the machining conditions as well as the cutting edge segments S_α and S_γ. Furthermore, this paper presents the influence of tailored cutting edges on tool wear, burr formation and residual stresses in slot milling of 42CrMo4 steel regarding the normalized ploughing zone in front of the cutting edge.

Keywords: Milling, Cutting Edge Microgeometry, Wear, Force, Surface Integrity

1. Introduction

In industrial production a high productivity and especially high process reliability of machining processes is of great importance. In this context the microgeometry of the cutting edge is one factor that influences the tool wear and therefore tool life, process reliability and workpiece quality. Consequently many research activities analyze the preparation process, the characterization of the honed cutting edge as well as the resulting performance of prepared tools in different machining applications.

Microblasting, abrasive brushing, magnet- or drag-finishing, electro-erosion as well as laser techniques have been established to produce different types of cutting edge microgeometries. Each preparation method has its field of application depending on its productivity, reproducibility and flexibility in terms of the size and the form of the required hone [1, 2, 3, 4]. The design of the cutting edge has a major influence on the process forces, the temperature and therefore on the resulting tool wear and surface integrity [5, 6, 7]. These effects are strongly connected with the so called ploughing in front of the cutting edge, whereas the ploughing forces are significantly affected by the size of the honed cutting and therefore by the undeformed chip thickness h in the area of the hone [8, 9].

To analyze the effect of the cutting edge micro-geometry on the performance of cutting tools systematically, the constitution of its microgeometry is a fundamental requirement. For this reason different fitting algorithms and characterization methods have been proposed in the past [10, 11, 12, 13].
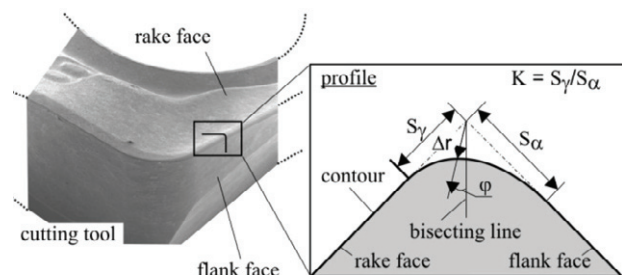

Figure 1: Characterization of the cutting edge micro geometry [13]

In this work the cutting edge segments S_γ, S_α and the form factor $K = S_\gamma / S_\alpha$ (Figure 1) have been applied in

order to constitute symmetric as well as asymmetric hone designs of the cutting edge microgeometry [13].

Nomenclature

A'_α	normalized ploughing zone
A_α	ploughing zone
b_w	burr width
CH	chipping wear
h	undeformed chip thickness
h_S	undeformed chip thickness in the hone
KT	face wear
l_α	contact length on flank face
l_γ	contact length on rake face
P_α	contact point on flank face
P_γ	separation point on rake face
S	stagnation point
S_α	cutting edge segment on flank face
S_γ	cutting edge segment on rake face
T	tool life
VB	flank wear
Δr	cutting edge flattening
K	form factor of the hone
α	clearance angle
γ	rake angle
γ_{eff}	effective rake angle
φ	inclination angle of the hone
σ	residual stresses
τ_{max}	depth of penetration

2. Characterization of honed cutting edges

In order to investigate the cutting performance of tools with tailored cutting edges, the characterization of the hone has to be applied to the orientation of the tool regarding the clearance and rake angle of the cutting process, as published in [12]. One parameter that considers the tool orientation is the undeformed chip thickness h_S in the area of the hone (Figure 2). This parameter can be described as the fraction of the undeformed chip thickness h below the stagnation point S flowing in the direction of the workpiece while the material above this point is sheared off. Even for the

same undeformed chip thickness in the hone h_S, different designs of the cutting edge microgeometry induce a unique tool wear behavior. Therefore more detailed parameters of the cutting edge in consideration of the tool orientation are necessary.
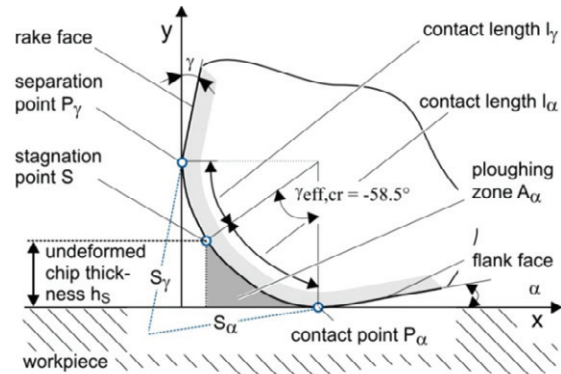

Figure 2: Characterization of the cutting edge

For this purpose, the following parameters have been defined (Figure 2). The profile of the cutting edge is orientated considering the clearance angle α and the rake angle γ of the cutting process. The contact point P_α with the machined surface is identified. Following the hone, the stagnation point S appears at an effective rake angle between $\gamma_{eff} = -57$ and $-65°$ [14, 15]. In this work the effective rake angle of the stagnation point S has been set to $\gamma_{eff} = -58.5°$, according to the results of Woon [14]. The third characteristic point along the hone is the separation point P_γ on the rake face. From this point on the rake angle remains constant, due to the macro geometry of the tool. The contact length l_γ between P_γ and S has a great influence on the chip flow due to the high negative effective rake angle. Consequently, the contact length l_α is the distance between S and the contact point P_α, whereas l_α is supposed to have a major influence on the friction between the hone and the workpiece and therefore on the process forces and surface integrity. A suitable parameter that is able to model the influence of the hone design on the cutting process is the area between the cutting edge profile and the workpiece bordered within S and P_α. This parameter can be defined as the ploughing zone A_α (Equation 1).

$$A_\alpha = \int_{S}^{P\alpha} P(x)dx$$

(1)

Taking into account, that two different designs of the microgeometry may have the same ploughing zone A_α and that the contact length l_α is supposed to have a major effect on the friction between the workpiece and the tool, this A_α is applied to the contact length l_α and therefore normalized as defined in equation 2.

$$A'_\alpha = \frac{A_\alpha}{l_\alpha} \qquad (2)$$

The normalized ploughing zone A'_α considers the undeformed chip thickness in the hone h_S as well as the contact length l_α and therefore the unique design of honed cutting edges in respect of the tool orientation in the cutting process.

### 3. Cutting performance in slot milling of 42CrMo4 steel

In the following the cutting performance of tools with tailored cutting edges will be examined in slot milling of 42CrMo4-QT steel with respect to the surface integrity of the machined workpiece in correlation to the normalized ploughing zone A'_α.

Experimental setup

Table 1: Variation of cutting edge microgeometry

Type	Ref.	I	II	III	IV	V	VI	VII	VIII
K			1				1.5		0.5	
S_α	10	20	30	40	60	20	30	40	60
S_γ	10	20	30	40	60	40	60	20	30

Cemented carbide cutting tools with different designs of the cutting edge microgeometry have been prepared by means of abrasive brushing. The performance of these cutting tools will be analyzed during slot milling of 42CrMo4-QT steel. The systematical variation of the microgeometry is presented in Table 1. Four symmetric hones with a form factor of $K = 1$ as well as two asymmetric hones with $K = 0.5$ and respectively $K = 1.5$ are applied. Unprepared, sharp tools will be used as a reference.
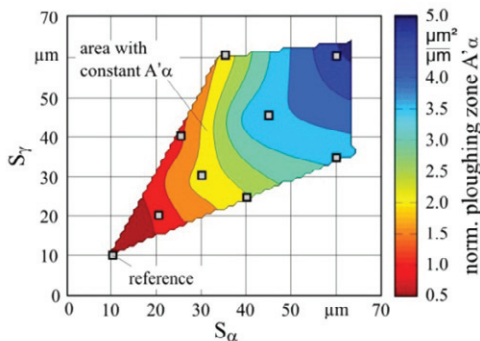
Tool:
type: ADGT 080308R
company: Walter AG
substrat: cemented carbide

Preparation:
method: abrasive brushing
type: SiC#240

Figure 3: Normalized ploughing zone A'_α

Figure 3 illustrates the normalized ploughing zone A'_α for all prepared cutting tools. The square icons in the diagram represent the desired hone design. To create this map as well as the following tool life map, the current values of 18 honed cutting edges have been used. Due to the deviation of the brushing process of approximately 7 %, the map does not fit perfectly to the icons. The contour plot illustrates, that the normalized ploughing zone A'_α increases for symmetric as well as asymmetric hone design with a form factor of $K < 1$. Due to this, the cutting edge segment S_α can be identified as the main factor on the normalized ploughing zone, whereas an increase of the cutting edge segment S_γ causes no significant influence, when S_α remains constant.

The experiments have been conducted with a single-tooth milling cutter with a diameter of $D = 25$ mm at a constant cutting speed of $v_c = 230$ m/min, a feed per tooth of $f_z = 0.2$ mm and a depth of cut of $a_p = 0.15$ mm. The cutting tools of the type ADGT 080308R-F56 were coated with a PVD TiAlN-Al$_2$O$_3$ hard coating. The cutting experiments were carried out on a HELLER 4-Axes Machining Centre MC16 without coolant.

Tool life and wear behavior

The results of the cutting experiments are illustrated by means of tool life maps as shown in figure 3. These maps illustrate changes in tool life due to different designs of the cutting edge microgeometry in relation to unprepared sharp reference tools [6]. Tool life criteria have been defined as the maximum flank wear of $VB_{max} = 100$ µm, face wear $KT_{max} = 60$ µm or chipping of the cutting edge $CH_{max} = 60$ µm [16]. The wear detection has been carried out using a digital microscope Keyence VHX-600.
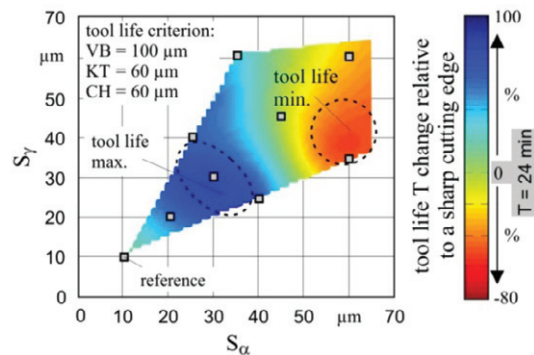
Tool:
type: ADGT 080308R
company: Walter AG
substrat: cemented carbide
coating: TiAlN+Al$_2$O$_3$
diameter: $D = 25$ mm
no. of teeth: $z = 1$

Process:
cutting speed: $v_c = 230$ m/min
depth of cut: $a_p = 1.5$ mm
feed per tooth: $f_z = 0.2$ mm
width of cut: $a_e = 25$ mm
cooling: none
material: 42CrMo4-QT

Figure 4: Tool life map of 42CrMo4 steel

As a result, cutting edges with sharp and small symmetric hones with $S_\alpha = S_\gamma = 20\ \mu m$ show initial chipping wear after a short time of cut. Increasing the size of the symmetric hone as well as the one with $K > 1$ leads to a domination of face wear KT. The major depth of the face wear occurs at the intersection with the cutting edge. As specified in [16], this kind of wear can be described as stair-formed rake face wear and is a result of the high thermo-mechanical load induced by the negative effective rake angle in the area of the contact length $l\gamma$.
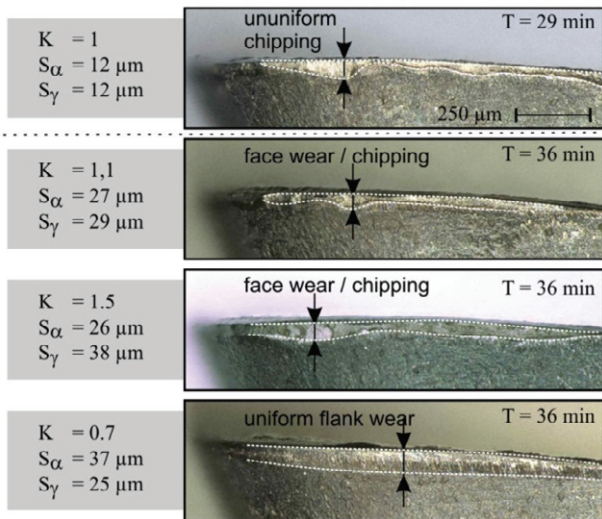

Figure 5: Characteristic tool wear

The area of maximum tool life of $T \approx 48$ min is between $S_\alpha = S_\gamma\ 30\pm5\ \mu m$ for $K \leq 1$ as well as $K \geq 1$, while the wear behavior in this area is changing from face wear ($K \geq 1$) to flank wear ($K \leq 1$) as shown in figure 4 at a time of cut of $T = 36$ min. With a further increase of S_α the flank wear dominates and the tool life decreases by reaching the tool life criterion of $VB_{max} = 100\ \mu m$. This can be explained with the higher contact length of the cutting edge with the workpiece at the flank face. The contact length by $S_\alpha = 30\ \mu m$ is equal to $l_\alpha = 27\ \mu m$, whereas it becomes $l_\alpha = 49\ \mu m$ by $S_\alpha = 60\ \mu m$. This leads to an increase of friction between the flank face and the workpiece.

Process forces

The process forces have been measured using a multicomponent dynamometer Kistler type 9257B. The measured forces of the workpiece coordinate system have been transformed into the tool system to analyze the cutting force F_c, the cutting normal force F_{cN} and the passive force F_p. Figure 6 displays the process forces for the investigated cutting geometries in correlation with the normalized ploughing zone A'_α.

The cutting force F_c as well as the cutting normal force F_{cN} increase by increasing the normalized ploughing zone A'_α. By shifting the cutting edge hone in the direction of the flank ($K < 1$) or rake face ($K > 1$) A'_α decreases relatively symmetric hone designs and therefore the forces decline. The passive force F_p remains almost constant with an increase of A'_α. The propagation of the cutting force F_c and cutting normal force F_{cN} is due to the fact, that the material below the stagnation point S becomes compressed between the workpiece and the cutting tool. This ploughing effect correlates with the applied ploughing zone for different types of tailored cutting edges.
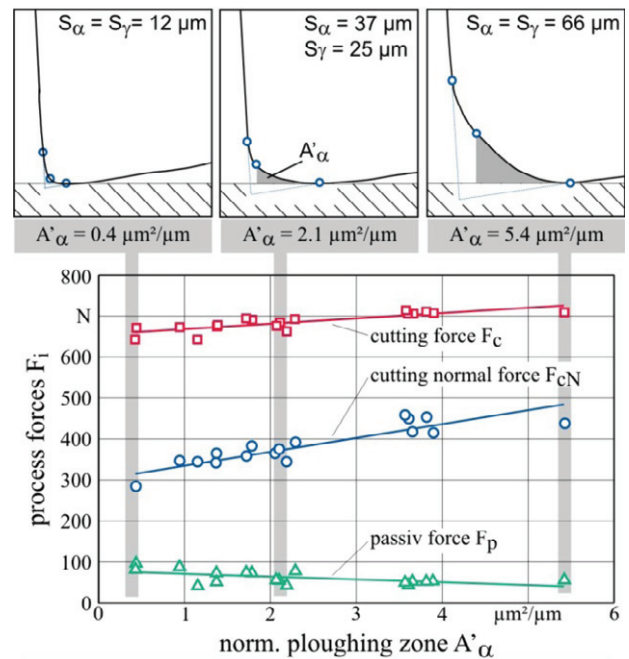
Tool:		Process:	
type:	ADGT 080308R	cutting speed:	$v_c = 230$ m/min
company:	Walter AG	depth of cut:	$a_p = 1.5$ mm
substrat:	cemented carbide	feed per tooth:	$f_z = 0.2$ mm
coating:	TiAlN+Al$_2$O$_3$	width of cut:	$a_e = 25$ mm
diameter:	$D = 25$ mm	cooling:	none
no. of teeth:	$z = 1$	material:	42CrMo4-QT

Figure 6: Process forces

Burr formation and surface integrity

The burr formation has been characterized by measuring the burr width of the top burr orthogonal to the feed direction. Chern classified burr types in five classes: 1) the knife-type-burr, 2) the wave-type burr, 3) the curl-type burr, 4) the edge-breakout and 5) the secondary burr [17].

Analog to the process forces the burr width increases by an increase of the symmetric cutting edge hone due to a larger normalized ploughing area A'_α and decreases

again by using asymmetric rounded cutting edges, where A'$_\alpha$ decreases.
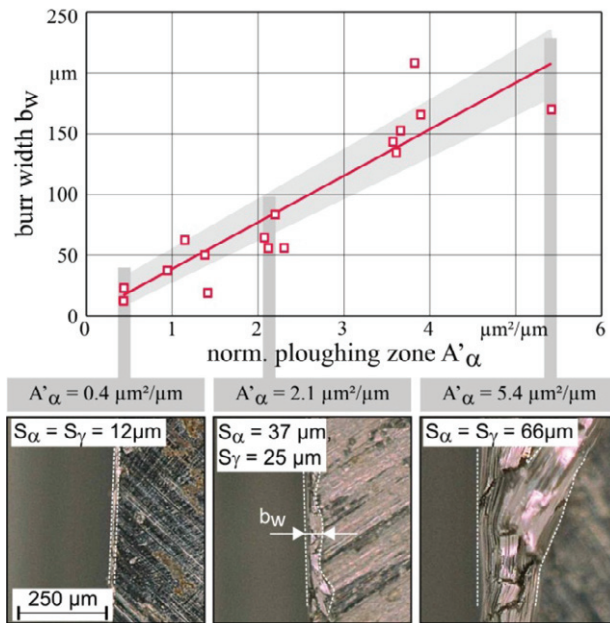

Figure 7: Burr formation

According to the classification of Chern the top burr type changes from knife-type, for sharp cutting edges, to curl-type for rounded cutting edges (Figure 8). The bigger the normalized ploughing zone A'$_\alpha$ the more irregular is the burr formation. For cutting edges with A'$_\alpha$ > 4 µm²/µm wave-type burr formation can be observed and therefore the burr width deviation increases.
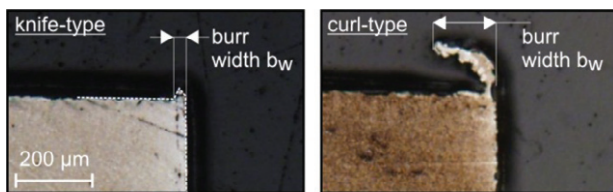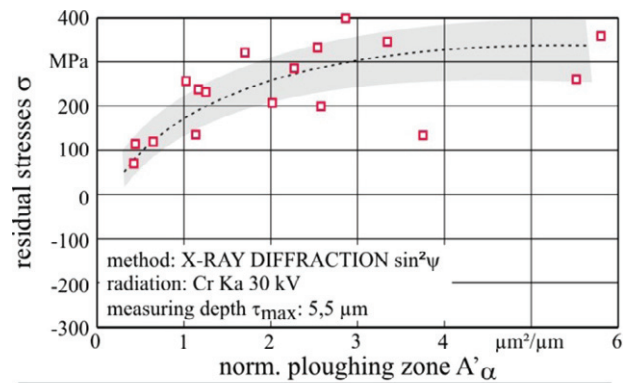

Figure 8: Knife-type and curl-type burr

As the design of the cutting edge hone influences the material flow and therefore the process forces and burr formation, the residual stresses have been measured in the flank surface of the machined slot using X-ray diffraction with the sin²ψ method (Figure 9).

The measured data represents the value of the residual stresses in a depth of τ_{max} = 5,5 µm. Sharp cutting edges as well as a hone design with a low normalized ploughing zone A'$_\alpha$ show tensile stresses in a range of σ = 100-200 MPa. As A'$_\alpha$ increases by the variation of the hone design, high tensile residual

stresses up to σ = 350-400 MPa occur. The effect of the residual stresses is due to the fact, that the hone design of the cutting edge causes a material displacement and therefore a unique thermo-mechanical load. The bigger the normalized ploughing zone A'$_\alpha$ the more material flows between the tool and the workpiece, which can be seen by the burr formation (Figure 7) and process forces (Figure 6). As it has been reported in [6] the temperature in the cutting zone increases as the cutting edge segment S$_\alpha$ increases. As a result the observed tensile stresses are a combination of the thermal load and the plastic-elastic deformation of the subsurface due to the material displacement.

Figure 9: Residual stresses

4. Conclusion

Tailored cutting edge microgeometries enhance the tool life significantly due to changes of the characteristic tool wear behavior. To investigate the cutting performance of tools with honed cutting edges, a new parameter has been presented, which allows describing different types of cutting edges in consideration of the machining conditions. The tool life of sharp cutting edges is limited by chipping wear, while the maximum of tool life is between S$_\alpha$ = S$_\gamma$ 30±5 µm for K ≤ 1 as well as K ≥ 1. The wear behavior of honed cutting edges shows a strong connection to the form factor K. Shifting the hone to the rake face, face wear occur due to the negative effective rake angle in the hone. Changing the hone design to a form factor of K < 1 flank wear dominates due to an increase of friction between the tool and the workpiece. The normalized ploughing zone A'$_\alpha$ shows a good correlation between cutting force F$_c$ and the cutting normal force F$_{cN}$, burr formation and residual stresses and can therefore be applied for different

designs of the cutting edge microgeometries in order to quantify the mechanical load of the tool and the subsurface of the workpiece.

Future investigations will concentrate on the influence of different workpiece materials on the hone design of cutting tools as well on the residual stress depth distribution in respect to the normalized ploughing zone A'_α for tailored cutting edges.

Acknowledgements

References

[1] Biermann, D, Terwey I. Cutting Edge Preparation to Improve Drilling Tools for HPC Processes. In: CIRP Journal of Manufacturing Science and Technology, 1/2; 2008, p. 76-80

[2] Denkena B, de Leon-García L, Bassett E, Rehe M. Cutting Edge Preparation by Means of Abrasive Brushing. In: 8th International Conference "THE Coatings" in Manufacturing Engineering. Erlangen: Key Engineering Materials, Vol. 438; 2010, p. 1-7

[3] Aurich JC, Zimmermann M, Leitz L. The preparation of cutting edges using a marking laser. In: Production Engineering, 5(1), Springer Verlag; 2010, p. 17-24

[4] Yussefian NZ, Koshy P, Buchholz S, Klocke F. Electro-erosion edge honing of cutting tools. In: CIRP Annals – Manufacturing Technology, 59(1); 2010, p. 215-218

[5] Biermann D, Baschin A. Influence of cutting edge geometry and cutting edge radius on the stability of micromilling processes. In: Production Engineering, 3, Springer Verlag; 2009, p. 375-380

[6] Denkena B, Lucas A, Bassett E. Effects of the cutting edge microgeometry on tool wear and its thermomechanical load. In: CIRP Annals – Manufacturing Technlogy, 60(1); 2011, p. 73-76

[7] Thiele JD, Melkote SN. Effect of Cutting-Edge Geometry and Workpiece Hardness on Surface Residual Stresses in Finish Hard Turning of AISI 52100 Steel. In: ASME, Vol. 122 (4); 2000, p. 642-649

[8] Albrecht P. New Developments in the Theory of the Metal-Cutting Process. In: ASME Transactions, Journal of Engineering for Industry, Series B, Vol. 82; 1960, p. 348-358

[9] Guo YB, Chou YK. The determination of ploughing force and its influence on material properties in metal cutting. In: Journal of Matetrials Processing Technology, 148; 2004, p. 368-375

[10] Wyen CF, Knapp W, Wegener K. A new method for the characterization of rounded cutting edges. In: The Internationalm Journal of Advanced Manufacturing Technology, Online First™, 2 September 2011

[11] Tikal F, Bienemann R, Heckmann L. Schneidkantenpräparation Ziele, Verfahren und Messmethoden. Franz Tikal, 2009

[12] Cortés Rodriguez CJ. Cutting edge preparation of precision cutting tools by applying micro-abrasive jet machining and brushing. In: PhD Thesis, Universität Kassel, 2009

[13] Denkena B, Reichstein M, Brodehl J, de León García L. Surface Preparation, coating and wear performance of geometrically defined cutting edges. In: Proceedings of the 5th International Conference "THe Coatings" in Manufacturing Engineering, 5-7; October 2005

[14] Woon KS, Rahman M, Neo KS, Liu K. The effect of tool edge radius on the contact phenomenon of tool-based micromachining. In: International Journal Of Machine Tools & Manufacture, 48; 2008, p. 1395-1407

[15] Yen Y-C, Jain A, Altan T. A finite element analysis of orthogonal machining using different tool edge geometries. In: Journal of Materials Processing Technology, 146, 2004, p. 72-81

[16] ISO 8688-2. Tool life testing in milling – Part 2: End milling. 1989

[17] Chern GL. Analsys of Burr Formation and Breakout in Metal Cutting. In: PhD Thesis, University of California of Berkely, 1993